DALTON
FULL PAPER

Dinuclear nickel(II) complexes with a tridentate nitrito bridge and terminal thiocyanato ligands. Crystal structure and magnetic properties

Albert Escuer,[a] Mercè Font-Bardía,[b] Evaristo Peñalba,[a] Núria Sanz,[a] Xavier Solans[b] and Ramon Vicente*[a]

[a] *Departament de Química Inorgànica, Universitat de Barcelona, Diagonal 647, 08028-Barcelona, Spain. E-mail: rvicente@kripto.qui.ub.es*
[b] *Departament de Cristal.lografia i Mineralogia, Universitat de Barcelona, c/Martí Franques s/n, 08028-Barcelona, Spain*

Received 11th May 1999, Accepted 9th July 1999

The μ-(η^1-*N*:η^2-*O*,*O*)-nitrito dinuclear compounds $[Ni_2(\mu\text{-}NO_2)(NCS)_3(Medpt)_2]\cdot H_2O$ **1** and $[Ni_2(\mu\text{-}NO_2)(NCS)_3(dpt)_2]$ **2**, and the mononuclear nitrito compounds $[Ni(NO_2)(NCS)(Medpt)]$ **3** and $[Ni(NO_2)(NCS)(Medien)]$ **4**, where Medpt = bis(3-aminopropyl)methylamine, dpt = bis(3-aminopropyl)amine and Medien = bis(2-aminoethyl)methylamine, have been synthesized and characterised. The crystal structures of **1**–**4** have been determined by single-crystal X-ray analysis. The thiocyanate ligand appears to stabilise the tridentate co-ordination mode of the nitrito ligand. The magnetic behaviour of the dinuclear compounds **1** and **2** was recorded between 300 and 4 K, showing antiferromagnetic coupling in both cases. The magnetic susceptibility data were fitted by the expression for a dinuclear nickel(II) compound giving the parameters $J = -12.8$ cm^{-1}, $g = 2.17$ and $J = -12.2$ cm^{-1}, $g = 2.27$ for **1** and **2** respectively.

In a previous study on the bridging carbonate ligand we structurally and magnetically characterised one new pentadentate co-ordination mode for this ligand in the trinuclear compound $[Ni_3(Medpt)_3(NCS)_4(\mu_3\text{-}CO_3)]$. This was obtained by mixing with the carbonate ligand, the nickel(II) salt and the Medpt ligand [bis(3-aminopropyl)methylamine], another potentially bridging ligand, thiocyanate, which in this case acts as a terminal ligand.[1] In this compound the thiocyanate anion is critical to the synthesis: all the attempts to synthesize the similar trinuclear compound from halides or different pseudohalide ligands were unsuccessful, because extremely soluble compounds (oils or gums) were obtained. The very similar selenocyanate anion also allows isolation of the compound $[Ni_3(Medpt)_3(NCSe)_4(\mu_3\text{-}CO_3)]$.[2]

Can the thiocyanate anion play the same synthetic role with other potentially bridging ligands? In an attempt to answer this question we used the same synthetic strategy for the nitrito anion. We obtained two new dinuclear μ-NO_2 compounds: $[Ni_2(\mu\text{-}NO_2)(NCS)_3(Medpt)_2]\cdot H_2O$ **1** and $[Ni_2(\mu\text{-}NO_2)(NCS)_3(dpt)_2]$ **2** [dpt = bis(3-aminopropyl)amine]. Here the thiocyanate also acts as a terminal ligand and the nitrito as a tridentate bridging ligand by using a co-ordination mode not found previously in a dinuclear nickel(II) compound, but recently reported in one mixed valence dicopper(I,II) compound, one copper(I)–zinc(II) analogue[3] and in a nickel–manganese bimetallic chain.[4] This bridging network involves a monodentate(N) *nitro* co-ordination with respect to one Ni^{II} and a bidentate(O,O′) *nitrito* co-ordination with respect to the other Ni^{II}. The octahedral co-ordination polyhedron for each nickel(II) is completed by the three nitrogen atoms of one tridentate amine and, due to the asymmetrical co-ordination mode of the bridging ligand, by two thiocyanate terminal ligands in the *nitro*nickel(II) and one thiocyanate terminal ligand in the *nitrito*nickel(II).

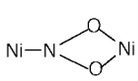

In the synthesis the triamine used and the stoichiometric ratio between the nickel(II) salt, triamine, thiocyanate salt and sodium nitrite influence the final product: with bis(3-aminopropyl)methylamine only the ratio 1:1:1:1 allowed the synthesis of the dinuclear compound **1**, whereas the theoretical ratios 2:2:3:1 and 1:1:2:1 allowed the synthesis of the mononuclear compound $[Ni(NO_2)(NCS)(Medpt)]$ **3**. With bis(3-aminopropyl)amine the dinuclear compound **2** was obtained with different ratios, but with Medien [bis(2-aminoethyl)methylamine] it was not possible to obtain the dinuclear product and only the mononuclear compound $[Ni(NO_2)(NCS)(Medien)]$ **4** was obtained.

Experimental

Synthesis

$[Ni_2(\mu\text{-}NO_2)(NCS)_3(Medpt)_2]\cdot H_2O$ 1. This was prepared by mixing 2.65 mmol of nickel(II) nitrate hexahydrate in 15 ml of water, 2.65 mmol of sodium nitrite in 5 ml of water, 2.65 mmol of potassium thiocyanate in 5 ml of water and 2.65 mmol of Medpt. After 1 h of stirring the resulting blue solution was left to evaporate in air. Three days later violet monocrystals of complex **1** suitable for X-ray determination were collected (Found: C, 31.6; H, 6.2; N, 21.9; S, 14.6. Calc. for $C_{17}H_{38}N_{10}Ni_2O_3S_3$: C, 31.6; H, 6.2; N, 21.7; S, 14.9%).

$[Ni_2(\mu\text{-}NO_2)(NCS)_3(dpt)_2]$ 2. This was prepared by mixing 5.5 mmol of nickel(II) perchlorate hexahydrate, 5.5 mmol of dpt, 5.5 mmol of sodium nitrite and 5.5 mmol of ammonium thiocyanate in 150 ml of water. After 1 h of stirring the solution was filtered and the resulting blue solution left to evaporate in air. Several days later, violet monocrystals of complex **2** suitable for X-ray determination were collected (Found: C, 30.3; H, 5.8; N, 23.5; S, 16.3. Calc. for $C_{15}H_{34}N_{10}Ni_2O_2S_3$: C, 30.0; H, 5.7; N, 23.3; S, 16.0%).

$[Ni(NO_2)(NCS)(Medpt)]$ 3. This was prepared by mixing 2.65 mmol of nickel(II) nitrate hexahydrate in 15 ml of water, 5.30

Table 1 Crystal data and structure refinement for $[Ni_2(\mu\text{-}NO_2)(NCS)_3(Medpt)_2]\cdot H_2O$ **1**, $[Ni_2(\mu\text{-}NO_2)(NCS)_3(dpt)_2]$ **2**, $[Ni(NO_2)(NCS)(Medpt)]$ **3** and $[Ni(NO_2)(NCS)(Medien)]$ **4**

	1	**2**	**3**	**4**
Formula	$C_{17}H_{38}N_{10}Ni_2O_3S_3$	$C_{15}H_{34}N_{10}Ni_2O_2S_3$	$C_8H_{19}N_5NiO_2S$	$C_6H_{15}N_5NiO_2S$
Formula weight	644.17	600.12	308.05	280.0
T/K	293(2)	293(2)	293(2)	293(2)
Crystal system	Orthorhombic	Monoclinic	Triclinic	Orthorhombic
space group	$Pbc2_1$	$P2_1/c$	$P\bar{1}$	$Pbca$
a/Å	8.501(3)	12.5568(6)	7.000(11)	11.401(6)
b/Å	14.73(2)	14.1199(6)	8.555(8)	10.956(3)
c/Å	24.099(4)	15.5747(7)	10.769(9)	18.876(12)
α/°			88.17(7)	
β/°		103.763(4)	88.08(9)	
γ/°			86.58(9)	
V/Å^3	3017(5)	2682.1(2)	643.1(13)	2358(2)
Z	4	4	2	8
D_c/g cm^{-3}	1.418	1.486	1.591	1.578
μ(Mo-Kα)/cm^{-1}	14.91	16.69	16.70	18.13
Data/restraints/parameters	3274/7/351	4714/0/426	3372/0/193	3196/0/197
$R1$	0.0518	0.0337	0.0466	0.0317
$wR2$	0.1007	0.0851	0.1200	0.0744

mmol of sodium nitrite in 5 ml of water, 2.65 mmol of potassium thiocyanate in 5 ml of water and 2.65 mmol of Medpt. After 1 h of stirring the resulting deep blue solution was left to evaporate in air. Three days later deep blue monocrystals of complex **3** suitable for X-ray determination were collected (Found: C, 30.8; H, 6.2; N, 22.7; S, 10.2. Calc. for $C_8H_{19}N_5NiO_2S$: C, 31.2; H, 6.2; N, 22.7; S, 10.4%).

[Ni(NO$_2$)(NCS)(Medien)] 4. This was prepared by mixing 1.45 mmol of nickel(II) perchlorate hexahydrate in 20 ml of water, 1.45 mmol of Medien, 5.80 mmol of sodium nitrite in 5 ml of water and 1.45 mmol of ammonium thiocyanate in 5 ml of water. After 1 h of stirring the resulting blue solution was left to evaporate in air. Six days later blue crystals of complex **4** were obtained. Blue monocrystals suitable for X-ray determination were obtained from recrystallisation in DMF (Found: C, 25.3; H, 5.4; N, 25.2; S, 10.9. Calc. for $C_6H_{15}N_5NiO_2S$: C, 25.7; H, 5.4; N, 25.0; S, 11.5%).

Magnetic measurements

Magnetic susceptibility measurements in the temperature range 300–4 K were carried out on polycrystalline samples with a pendulum type magnetometer (MANICS DSM8) equipped with a helium continuous-flow cryostat and a Brucker B E15 electromagnet. The magnetic field was *ca.* 1.5 T. Diamagnetic corrections were estimated from Pascal's constants.

X-Ray crystallography

Prismatic violet crystals for complexes **1** and **2**, and prismatic blue crystals for **3** and **4**, were selected and mounted on an Enraf-Nonius CAD4 diffractometer for **1**, **3** and **4**, and on a STOE STADI4 diffractometer for **2**. Unit cell parameters were determined from automatic centring of 25 reflections ($12 < \theta < 21°$) for **1**, **3** and **4**, and of 56 reflections ($12.5 < \theta < 16.6°$) for **2**, and refined by the least-squares method. Intensities were collected with graphite monochromatised Mo-Kα radiation, using the ω–2θ scan technique. For **1** 3432 reflections were measured and 2779 assumed as observed, [$I > 2\sigma(I)$], for **2** 4945 reflections measured and 3435 observed [$I > 4\sigma(I)$], for **3** 3448 reflections measured and 3263 observed [$I > 2\sigma(I)$], and for **4**, 5974 reflections measured and 2979 observed [$I > 2\sigma(I)$]. Three reflections were measured every two hours as orientation and intensity control; no significant intensity decay was observed. The crystallographic data, conditions used for the intensity data collection and some features of the structure refinement are listed in Table 1. Lorentz-polarization, but not absorption, corrections were made for **1**, **3** and **4**, and absorption corrections with the ψ scan method were made for **2**.

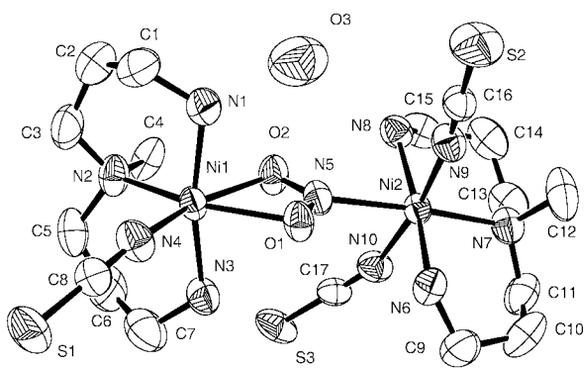

Fig. 1 An ORTEP drawing with the atom-labelling scheme for $[Ni_2(\mu\text{-}NO_2)(NCS)_3(Medpt)_2]\cdot H_2O$ **1**.

The crystal structures were solved by direct methods for complexes **1**, **3** and **4** and by Patterson synthesis for **2** using the SHELXS 86 computer program[5] and refined by the full-matrix least-squares method with the SHELXL 93 computer program.[6] The values of f, f' and f'' were taken from ref. 7. Six H atoms for **1**, 34 for **2**, 11 for **3** and 15 for **4** were located from a difference synthesis, and 25 for **1** and 8 for **3** were computed; all of them were refined with an overall isotropic factor using a riding model.

CCDC reference number 186/1567.

See http://www.rsc.org/suppdata/dt/1999/3115/ for crystallographic files in .cif format.

Results and discussion

Crystal structure

[Ni$_2$(μ-NO$_2$)(NCS)$_3$(Medpt)$_2$]·H$_2$O 1. Selected bond lengths and bond angles are given in Table 2. An ORTEP[8] drawing of the dinuclear unit with atom-labelling scheme is presented in Fig. 1. Complex **1** is a μ-(η^1-*N*:η^2-*O*,*O*)-nitrito dinuclear compound: the tridentate nitrito bridging ligand comprises a bidentate *nitrito*(O,O′) co-ordination with respect to Ni(1) and a monodentate *nitro*(N) co-ordination with respect to Ni(2). The octahedral co-ordination polyhedron for Ni(1) is completed by the three nitrogen atoms of one Medpt amine and by the nitrogen atom of one thiocyanate ligand. For Ni(2) the octahedral co-ordination polyhedron is completed by the three nitrogen atoms of one Medpt amine and by the nitrogen atoms of two thiocyanate ligands. For Ni(1) two of the co-ordination sites are

Table 2 Selected bond lengths [Å] and angles [°] for $[Ni_2(\mu\text{-}NO_2)(NCS)_3(Medpt)_2]\cdot H_2O$ **1**

Ni(1)–N(4)	2.022(7)	Ni(1)–N(1)	2.077(7)
Ni(1)–N(3)	2.077(7)	Ni(1)–N(2)	2.103(7)
Ni(1)–O(2)	2.173(6)	Ni(1)–O(1)	2.208(5)
Ni(2)–N(10)	2.068(6)	Ni(2)–N(8)	2.078(7)
Ni(2)–N(6)	2.079(7)	Ni(2)–N(9)	2.080(6)
Ni(2)–N(7)	2.146(7)	Ni(2)–N(5)	2.230(7)
S(1)–C(8)	1.628(8)	S(2)–C(16)	1.638(7)
S(3)–C(17)	1.645(7)	O(1)–N(5)	1.268(8)
O(2)–N(5)	1.253(7)		
N(4)–Ni(1)–N(1)	94.0(3)	N(4)–Ni(1)–N(3)	91.0(3)
N(1)–Ni(1)–N(3)	168.5(3)	N(4)–Ni(1)–N(2)	95.8(3)
N(1)–Ni(1)–N(2)	93.5(3)	N(3)–Ni(1)–N(2)	96.3(3)
N(4)–Ni(1)–O(2)	162.4(2)	N(1)–Ni(1)–O(2)	84.5(3)
N(3)–Ni(1)–O(2)	87.6(3)	N(2)–Ni(1)–O(2)	101.8(2)
N(4)–Ni(1)–O(1)	104.8(2)	N(1)–Ni(1)–O(1)	86.3(2)
N(3)–Ni(1)–O(1)	82.4(2)	N(2)–Ni(1)–O(1)	159.4(2)
O(2)–Ni(1)–O(1)	57.7(2)	N(10)–Ni(2)–N(8)	90.9(3)
N(10)–Ni(2)–N(6)	91.2(3)	N(8)–Ni(2)–N(6)	172.2(3)
N(10)–Ni(2)–N(9)	170.8(3)	N(8)–Ni(2)–N(9)	88.1(3)
N(6)–Ni(2)–N(9)	88.6(3)	N(10)–Ni(2)–N(7)	91.7(3)
N(8)–Ni(2)–N(7)	95.5(3)	N(6)–Ni(2)–N(7)	92.0(3)
N(9)–Ni(2)–N(7)	97.5(2)	N(10)–Ni(2)–N(5)	84.7(3)
N(8)–Ni(2)–N(5)	86.7(3)	N(6)–Ni(2)–N(5)	86.0(3)
N(9)–Ni(2)–N(5)	86.1(2)	N(7)–Ni(2)–N(5)	175.9(2)
N(5)–O(1)–Ni(1)	93.0(4)	N(5)–O(2)–Ni(1)	95.2(4)
C(1)–N(1)–Ni(1)	117.3(5)	C(8)–N(4)–Ni(1)	156.2(6)
O(2)–N(5)–O(1)	113.9(6)	O(2)–N(5)–Ni(2)	123.1(5)
O(1)–N(5)–Ni(2)	122.6(4)	C(16)–N(9)–Ni(2)	172.1(6)
C(17)–N(10)–Ni(2)	152.5(6)	N(4)–C(8)–S(1)	178.4(7)
N(9)–C(16)–S(2)	178.9(8)	N(10)–C(17)–S(3)	178.6(7)

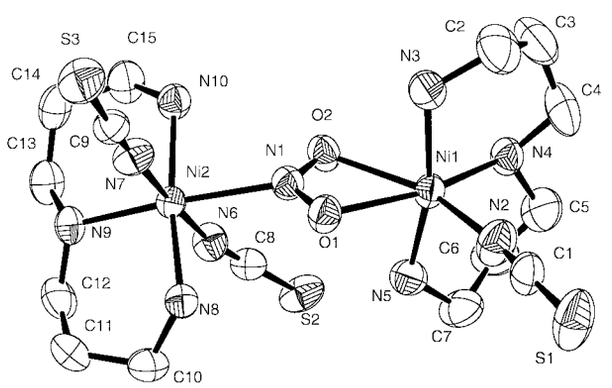

Fig. 2 An ORTEP drawing with the atom-labelling scheme for $[Ni_2(\mu\text{-}NO_2)(NCS)_3(dpt)_2]$ **2**.

occupied by two oxygen atoms of the nitrito bridging ligand: due to the O(2)–N(5)–O(1) angle of 113.9(6)°, Ni(1) is in a very distorted octahedral environment: O(1)–Ni(1)–O(2) 57.7(2), N(2)–Ni(1)–O(2) 101.8(2), N(4)–Ni(1)–O(1) 104.8(2)°. Atom Ni(2) has the monodentate *nitro*(N) co-ordination of the nitrito bridging ligand and, for this reason, the octahedral distortion is significantly smaller. It is in an elongated octahedral co-ordination with the four planar Ni–N distances in the range 2.068(6)–2.080(6) Å and Ni(2)–N(5) and Ni(2)–N(7) 2.230(7) and 2.146(7) Å respectively. The thiocyanate ligands are *trans* in the basal plane.

In complex **1** there is a non-co-ordinated water molecule. The shortest distances to this water molecule are intramolecular: O(3)···N(1), O(3)···S(2) and O(3)···S(1) are 3.034(6), 3.447(7) and 3.334(7) Å respectively.

$[Ni_2(\mu\text{-}NO_2)(NCS)_3(dpt)_2]$ 2. An ORTEP drawing of the dinuclear compound **2** with the atom-labelling scheme is shown in Fig. 2. The main bond lengths and bond angles are given in Table 3. The structure of **2** is like that of **1**. Only slight differences can be seen: in the bridging region the Ni(2)–N(1) 2.278(3) Å is longer than the Ni–N(*nitro*) distance in **1** (2.230(7) Å). The

Table 3 Selected bond lengths [Å] and angles [°] for $[Ni_2(\mu\text{-}NO_2)(NCS)_3(dpt)_2]$ **2**

Ni(1)–N(2)	2.007(3)	Ni(2)–N(6)	2.059(3)
Ni(1)–N(5)	2.056(4)	Ni(2)–N(10)	2.081(3)
Ni(1)–N(3)	2.075(3)	Ni(2)–N(7)	2.085(3)
Ni(1)–N(4)	2.086(3)	Ni(2)–N(8)	2.089(3)
Ni(1)–O(1)	2.204(2)	Ni(2)–N(9)	2.095(3)
Ni(1)–O(2)	2.291(2)	Ni(2)–N(1)	2.278(3)
S(1)–C(1)	1.624(4)	N(2)–C(1)	1.151(5)
S(2)–C(8)	1.634(4)	N(6)–C(8)	1.157(4)
S(3)–C(9)	1.637(3)	N(7)–C(9)	1.150(4)
O(1)–N(1)	1.264(3)	O(2)–N(1)	1.255(3)
N(2)–Ni(1)–N(5)	95.4(2)	O(1)–Ni(1)–O(2)	55.87(8)
N(2)–Ni(1)–N(3)	95.9(2)	N(6)–Ni(2)–N(10)	92.70(14)
N(5)–Ni(1)–N(3)	166.6(2)	N(6)–Ni(2)–N(7)	176.49(12)
N(2)–Ni(1)–N(4)	97.25(14)	N(10)–Ni(2)–N(7)	87.51(13)
N(5)–Ni(1)–N(4)	94.21(14)	N(6)–Ni(2)–N(8)	92.09(13)
N(3)–Ni(1)–N(4)	91.52(14)	N(10)–Ni(2)–N(8)	169.39(12)
N(2)–Ni(1)–O(1)	97.42(11)	N(7)–Ni(2)–N(8)	87.14(12)
N(5)–Ni(1)–O(1)	85.15(12)	N(6)–Ni(2)–N(9)	90.98(12)
N(3)–Ni(1)–O(1)	86.24(12)	N(10)–Ni(2)–N(9)	96.97(12)
N(4)–Ni(1)–O(1)	165.31(12)	N(7)–Ni(2)–N(9)	92.48(12)
N(2)–Ni(1)–O(2)	153.26(11)	N(8)–Ni(2)–N(9)	92.41(12)
N(5)–Ni(1)–O(2)	84.47(13)	N(6)–Ni(2)–N(1)	83.57(11)
N(3)–Ni(1)–O(2)	82.20(12)	N(10)–Ni(2)–N(1)	84.47(11)
N(4)–Ni(1)–O(2)	109.45(11)	N(7)–Ni(2)–N(1)	92.97(11)
N(8)–Ni(2)–N(1)	86.66(11)	N(2)–C(1)–S(1)	179.7(4)
N(1)–O(1)–Ni(1)	97.2(2)	N(6)–C(8)–S(2)	178.1(3)
N(1)–O(2)–Ni(1)	93.2(2)	N(7)–C(9)–S(3)	177.5(3)
C(1)–N(2)–Ni(1)	167.8(3)	N(9)–Ni(2)–N(1)	174.42(11)
C(8)–N(6)–Ni(2)	157.2(3)	O(2)–N(1)–Ni(2)	120.5(2)
C(9)–N(7)–Ni(2)	177.9(3)	O(1)–N(1)–Ni(2)	124.3(2)
O(2)–N(1)–O(1)	113.6(3)		

Ni–O(*nitrito*) distances are Ni(1)–O(1) 2.204(2) and Ni(1)–O(2) 2.291(2) Å (in **1** the same distances are 2.208(5) and 2.173(6) Å). The O(1)–N(1)–O(2) and O(1)–Ni(1)–O(2) angles are 113.6(3) and 55.87(8)° respectively (in **1** the same angles are 113.9(6) and 57.7(2)°).

$[Ni(NO_2)(NCS)(Medpt)]$ 3. Selected bond lengths and bond angles are given in Table 4. An ORTEP[8] drawing of the dinuclear unit with atom-labelling scheme is presented in Fig. 3. The nickel atom is in a distorted octahedral environment due to the geometry imposed by the bidentate nitrito-*O*,*O*′ ligand. The O(1)–Ni–O(2) angle is 57.48(11)°. Consequently, the other X–Ni–X (X = O or N) angles in the plane N(4)–N(5)–Ni–O(1)–O(2) are greater than 90°: O(1)–Ni–N(5) 106.13(12), O(2)–Ni–N(4) 103.03(12), N(5)–Ni–N(4) 93.33(12)°. If we consider the $Ni(O_2N)$ entity, all distances and angles are similar to the published values in analogous monuclear compounds.[9–15] The nitrito ligand and the terminal and central N-co-ordinated atoms of the *fac*-Medpt ligand are in the same plane.

$[Ni(NO_2)(NCS)(Medien)]$ 4. Selected bond lengths and bond angles are given in Table 5. An ORTEP drawing of the dinuclear unit with atom-labelling scheme is presented in Fig. 4. As in complex **3** the nickel atom is in a distorted octahedral environment due to the geometry imposed by the bidentate nitrito-*O*,*O*′ ligand. The O(1)–Ni–O(2) angle is 58.29(7)°. Consequently, the other X–Ni–X (X = O or N) angles in the plane N(3)–N(5)–Ni–O(1)–O(2) are greater than 90°: O(1)–Ni–N(3) 99.63(7), O(2)–Ni–N(5) 97.47(7) and N(3)–Ni–N(5) 104.30(8)°. If we consider the $Ni(O_2N)$ entity, all distances and angles are similar to the published values in analogous compounds[9–15] and the bond values found in **3**. In **4**, in contrast to **3**, the nitrito ligand and the two terminal N-co-ordinated atoms of the *fac*-Medien ligand are in the same plane.

Magnetic results

The plots of the magnetic susceptibility values per dimeric unit,

Table 4 Selected bond lengths [Å] and angles [°] for [Ni(NO_2)(NCS)(Medpt)] **3**

Ni–N(2)	2.042(3)	Ni–N(5)	2.045(3)
Ni–N(3)	2.062(3)	Ni–N(4)	2.087(3)
Ni–O(1)	2.156(3)	Ni–O(2)	2.166(4)
S–C(1)	1.623(3)	O(1)–N(1)	1.251(4)
O(2)–N(1)	1.244(3)	N(2)–C(1)	1.148(4)
N(2)–Ni–N(5)	90.46(13)	N(2)–Ni–N(3)	168.36(9)
N(5)–Ni–N(3)	94.51(13)	N(2)–Ni–N(4)	94.59(12)
N(5)–Ni–N(4)	93.33(12)	N(3)–Ni–N(4)	95.62(11)
N(2)–Ni–O(1)	84.45(13)	N(5)–Ni–O(1)	106.13(12)
N(3)–Ni–O(1)	84.07(12)	N(4)–Ni–O(1)	160.52(9)
N(2)–Ni–O(2)	85.76(13)	N(5)–Ni–O(2)	163.44(9)
N(3)–Ni–O(2)	86.51(12)	N(4)–Ni–O(2)	103.03(12)
O(1)–Ni–O(2)	57.48(11)	N(1)–O(1)–Ni	94.9(2)
N(1)–O(2)–Ni	94.7(2)	O(2)–N(1)–O(1)	112.8(2)
C(1)–N(2)–Ni	161.5(2)	N(2)–C(1)–S	179.1(2)

Table 5 Selected bond lengths [Å] and angles [°] for [Ni(NO_2)(NCS)(Medien)] **4**

Ni–N(1)	2.0416(15)	Ni–N(3)	2.0575(17)
Ni–N(5)	2.0741(18)	Ni–O(1)	2.1366(16)
Ni–N(4)	2.1439(14)	Ni–O(2)	2.1567(17)
S–C(1)	1.6309(17)	O(1)–N(2)	1.269(2)
O(2)–N(2)	1.255(2)	N(1)–C(1)	1.149(2)
N(1)–Ni–N(3)	92.63(6)	N(1)–Ni–N(5)	94.95(6)
N(3)–Ni–N(5)	104.30(8)	N(1)–Ni–O(1)	88.82(7)
N(3)–Ni–O(1)	99.63(7)	N(5)–Ni–O(1)	155.56(6)
N(1)–Ni–N(4)	175.22(7)	N(3)–Ni–N(4)	83.50(5)
N(5)–Ni–N(4)	83.33(5)	O(1)–Ni–N(4)	94.59(5)
N(1)–Ni–O(2)	90.43(7)	N(3)–Ni–O(2)	157.66(6)
N(5)–Ni–O(2)	97.47(7)	O(1)–Ni–O(2)	58.29(7)
N(4)–Ni–O(2)	94.21(5)	N(2)–O(1)–Ni	95.13(12)
N(2)–O(2)–Ni	94.60(12)	C(1)–N(1)–Ni	168.23(17)
O(2)–N(2)–O(1)	111.87(17)	N(1)–C(1)–S	178.47(16)

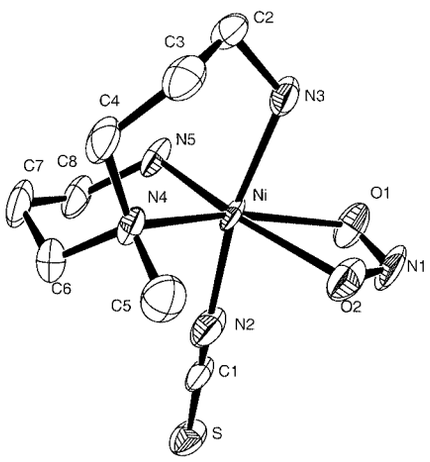

Fig. 3 An ORTEP drawing with the atom-labelling scheme for [Ni(NO_2)(NCS)(Medpt)] **3**.

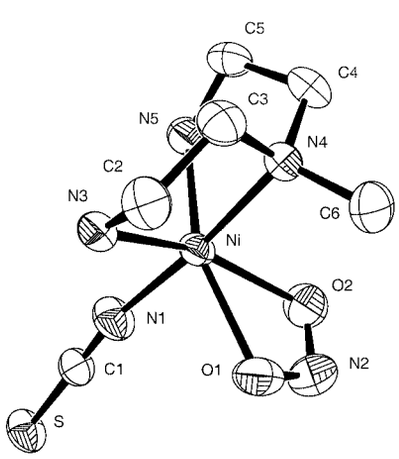

Fig. 4 An ORTEP drawing with the atom-labelling scheme for [Ni(NO_2)(NCS)(Medien)] **4**.

χ_m *vs.* T of [Ni_2(μ-NO_2)$(NCS)_3$(Medpt)$_2$]·H_2O **1** and [Ni_2(μ-NO_2)$(NCS)_3$(dpt)$_2$] **2**, are shown in Fig. 5. The shape of the plots is consistent with antiferromagnetic [NiNi] entities: the χ_m plots show maximum susceptibility at 19 K for **1** and at 15 K for **2**, whereas $\chi_m T$ values decrease continuously from room temperature ($\chi_m T$ values 2.4 cm^3 K mol^{-1}, for **1** and **2** respectively) and tend to zero at low temperatures.

Experimental data were fitted by the isotropic expression derived from the Hamiltonian $H = -JS_1S_2$ for [NiNi] pairs, eqn. (1), where $f(J,T)$ is $(2\exp(J/kT) + 10\exp(3J/kT))/(1 + 3\exp(J/kT) + 5\exp(3J/kT))$.

$$\chi_m = N\beta^2 g^2/kT \cdot f(J,T) \quad (1)$$

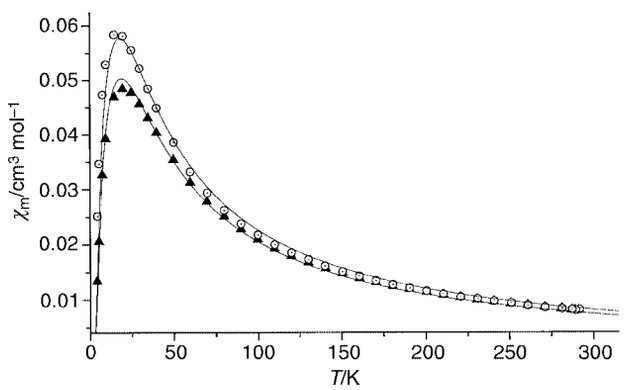

Fig. 5 Molar magnetic susceptibility *vs.* T plots of a polycrystalline sample of [Ni_2(μ-NO_2)$(NCS)_3$(Medpt)$_2$]·H_2O **1** (▲) and [Ni_2(μ-NO_2)-$(NCS)_3$(dpt)$_2$] **2** (○). Solid line shows the best fit using the expression for the magnetic susceptibility of isotropically coupled dinuclear $S = 1$ ions.

The criterion of best fit was the minimum value of $R = \Sigma_i(\chi_i^{calc} - \chi_i^{obsd})^2/(i - n)$, where n is the number of free parameters (3). The results of the fit, shown as the solid lines in Fig. 5, were $J = -12.8$ cm^{-1}, $g = 2.17$ for complex **1** and $J = -12.2$ cm^{-1}, $g = 2.27$ for **2**. It is interesting that the interaction through the same kind of μ-(η^1-*N*:η^2-*O*,*O*)-nitrito bridge in the Ni–Mn bimetallic chain [{$MnNi(NO_2)_4(en)_2$}$_n$] is ferromagnetic.[2] The similar values of the coupling constants found for **1** and **2** can be explained in terms of similar bond parameters in the bridging region.

Magneto-structural correlations

The lower value of the superexchange coupling constant for the O,O′,N nitrito bridge described in this paper, close to -12 cm^{-1}, in comparison with the well established value of J, close to -30 cm^{-1}, reported for the O,N nitrito bridge[16] is surprising. The co-ordination of the second oxygen atom seems to afford an increase in the overlap in the bridging region and this suggests a strong interaction, in contrast with experimental results.

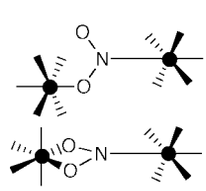

This experimental finding can be explained by reference to the Hay–Thibeault–Hoffmann relationship[17] between the $\Sigma\Delta^2$ and the antiferromagnetic contribution of J. The Δ values (difference of energy between active MOs of the same symmetry)

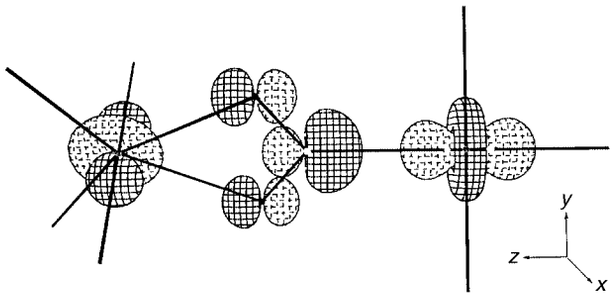

Fig. 6 Plot of one of the antibonding MOs involved in the superexchange pathway showing the axial–equatorial d_{z^2} interaction.

may easily be obtained by means of MO extended Hückel calculations by the CACAO program.[18] Calculations were performed on a dimeric model using as input parameters Ni–O and Ni–N (nitrito) distances 2.25 Å, O–N–O angle 114°, and the remaining co-ordination sites occupied by NH_3 molecules at a Ni–N distance of 2.075 Å.

The result of the calculation indicates that the two oxygen atoms mainly interact with the $d_{x^2-y^2}$ atomic orbital of one of the nickel atoms, whereas the nitrogen interacts with the d_{z^2} orbital of the second nickel atom. In Fig. 6 the plot of one of the antibonding MOs involved in the superexchange pathway is shown; this plot indicates strict orthogonality between the corresponding $d_{x^2-y^2}$ atomic orbitals, that is to say $\Delta^2 = 0$, and the only active pathway for the superexchange interaction should be between the two reversed d_{z^2} orbitals. If we compare the shape and orientation of the d_{z^2} orbitals for the two kinds of nitrito bridges, the lower $\Sigma\Delta^2$ and J values found for the O,O′,N co-ordination as a consequence of the reduction of the overlap are evident.

Acknowledgements

Financial support for this work was generously given by Dirección General de Investigación Científica y Técnica through Grant PB96/0163.

References

1 A. Escuer, R. Vicente, S. B. Kumar, X. Solans, M. Font-Bardía and A. Caneschi, *Inorg. Chem.*, 1996, **35**, 3094.
2 A. Escuer, M. S. El Fallah, S. B. Kumar, F. Mautner and R. Vicente, *Polyhedron*, 1998, **18**, 377.
3 J. A. Halfen, S. Mahapatra, E. C. Wilkinson, A. J. Gengenbach, V. G. Young, L. Que and W. B. Tolman, *J. Am. Chem. Soc.*, 1996, **118**, 763.
4 O. Kahn, E. Bakalbassis, C. Mathoniere, M. Hagiwara, K. Katsumata and L. Ouahab, *Inorg. Chem.*, 1997, **36**, 1530.
5 G. M. Sheldrick, SHELXS 86, *Acta Crystallogr.*, *Sect. A*, 1990, **46**, 467.
6 G. M. Sheldrick, SHELXL 93, University of Göttingen, 1993.
7 *International Tables of X-Ray Crystallography*, Kynoch Press, Birmingham, 1974, vol. IV, pp. 99–100 and 149.
8 C. K. Johnson, ORTEP, Report ORNL-3794, Oak Ridge National Laboratory, Oak Ridge, TN, 1965.
9 A. J. Finney, M. A. Hitchman, D. L. Kepert, C. L. Raston, G. L. Rowbotton and A. H. White, *Aust. J. Chem.*, 1981, **34**, 2177.
10 A. J. Finney, M. A. Hitchman, C. L. Raston, G. L. Rowbotton and A. H. White, *Aust. J. Chem.*, 1981, **34**, 2159.
11 A. J. Finney, M. A. Hitchman, C. L. Raston, G. L. Rowbotton and A. H. White, *Aust. J. Chem.*, 1981, **34**, 2113.
12 A. Escuer, R. Vicente and J. Ribas, *Transition Met. Chem.*, 1993, **18**, 478.
13 M. G. B. Drew, D. M. L. Goodgame, M. A. Hitchman and D. Rogers, *Chem. Commun.*, 1965, 477.
14 R. Birdy, D. M. L. Goodgame, J. C. McConway and D. Rogers, *J. Chem. Soc.*, *Dalton Trans.*, 1977, 1730.
15 M. J. Goldberg and R. E. Marsh, *Acta Crystallogr.*, *Sect. B*, 1979, **35**, 960.
16 A. Escuer, R. Vicente and X. Solans *J. Chem. Soc.*, *Dalton Trans.*, 1997, 531 and refs. therein.
17 J. P. Hay, J. C. Thibeault and R. Hoffmann, *J. Am. Chem. Soc.*, 1975, **97**, 4884.
18 CACAO, Computed Aided Composition of Atomic Orbitals, version 4.0, C. Mealli and D. M. Proserpio, *J. Chem. Educ.*, 1990, **67**, 3399.

Paper 9/03756J